

ZEUS: Zero-shot Embeddings for Unsupervised Separation of Tabular Data

Patryk Marszałek

Tomasz Kuśmierczyk*

Witold Wydmański

Jacek Tabor

Marek Śmieja*

Faculty of Mathematics and Computer Science
Jagiellonian University
Łojasiewicza 6, 30-348 Kraków, Poland

Abstract

Clustering tabular data remains a significant open challenge in data analysis and machine learning. Unlike for image data, similarity between tabular records often varies across datasets, making the definition of clusters highly dataset-dependent. Furthermore, the absence of supervised signals complicates hyperparameter tuning in deep learning clustering methods, frequently resulting in unstable performance. To address these issues and reduce the need for per-dataset tuning, we adopt an emerging approach in deep learning: zero-shot learning. We propose ZEUS, a self-contained model capable of clustering new datasets without any additional training or fine-tuning. It operates by decomposing complex datasets into meaningful components that can then be clustered effectively. Thanks to pre-training on synthetic datasets generated from a latent-variable prior, it generalizes across various datasets without requiring user intervention. To the best of our knowledge, ZEUS is the first zero-shot method capable of generating embeddings for tabular data in a fully unsupervised manner. Experimental results demonstrate that it performs on par with or better than traditional clustering algorithms and recent deep learning-based methods, while being significantly faster and more user-friendly.

1 Introduction

Clustering remains a fundamental yet challenging task in unsupervised learning. It is particularly hard for tabular data, which inherently lacks the structured spatial or semantic properties of images or texts. Unlike for image clustering, where intrinsic visual similarities can guide cluster formation, defining meaningful similarities in tabular data is highly dataset-specific, complicating the generalization of clustering methods across diverse applications. Recent developments leveraging deep learning have demonstrated promise in generating richer representations for clustering tasks. However, these methods frequently suffer from instability due to their sensitivity to hyperparameter selection, a challenge exacerbated by the absence of supervised signals to guide optimization. Consequently, practitioners working with tabular data often resort to simpler, classical algorithms like k-means, despite their limited capacity for capturing complex underlying data structures, simply to avoid extensive manual tuning.

We address these challenges with ZEUS – a zero-shot transformer-based model for embedding new tabular datasets in a form convenient for unsupervised separation (=clustering), without the need for additional fine-tuning. Given a new dataset, ZEUS returns its transformed representation, where

*Joint contribution to project conception, design, and research supervision.

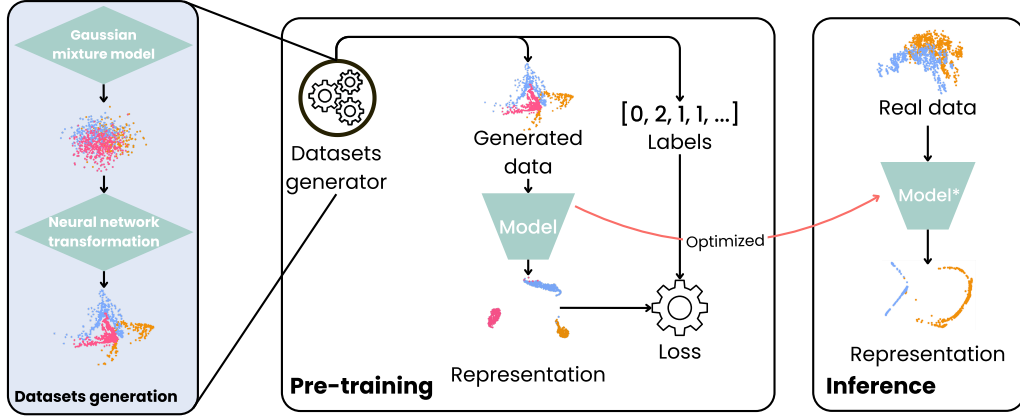


Figure 1: Schematic characterization of ZEUS: (left) synthetic datasets generation; (middle) pre-training on datasets with known labels; (right) deployment of a frozen model for real-world tasks.

clusters can be easily discovered using simple methods, like k-means. Since it works as a zero-shot learner, it significantly reduces hyperparameter tuning complexity and the computation time, enabling effective clustering in seconds. It is a plug-and-play solution that requires no fine-tuning and runs in a single forward pass for new datasets.

Inspiration for ZEUS stems from the Prior-data Fitted Networks (PFNs) [15], a recently introduced framework highlighting the potential of in-context learning for tabular data. PFNs operate by feeding a transformer contexts representing complete tasks, i.e., training data along with query samples for which the model predicts labels. Despite their impressive performance, they are limited to supervised problems. ZEUS extends this basic idea for unsupervised tasks by addressing the two key challenges of how to: (1) generate prior synthetic data with clear but non-trivial clustering structures for pre-training; and (2) encode prior clustering knowledge for new unlabeled datasets. Additionally, in contrast to TabPFN, ZEUS is a zero-shot model and during inference does not rely on any context labels.

Unlike traditional methods that optimize arbitrary heuristics (e.g., DEC), ZEUS approaches clustering by learning how to invert data generation processes. In particular, it is pre-trained on synthetic datasets to learn how to infer cluster assignments. The datasets have known latent structures, which enables supervised guidance for the training, and by generating diverse datasets we supply it with the prior knowledge about what can constitute a possible clustering structure, enabling effective generalization to new real-world datasets during inference. Figure 1 illustrates the key concepts of the method while Figure 2 presents representations generated by ZEUS.

Experiments demonstrate that ZEUS consistently matches or surpasses both classical clustering algorithms and recent deep learning-based approaches, establishing it as a powerful and practical tool for the unsupervised analysis of tabular data. Beyond its strong empirical performance, we also provide theoretical justification by showing that ZEUS fits the framework of Prior-data Fitted Networks, thereby reinforcing its theoretical soundness (see Section 2.3).

We supplement the paper with an appendix that includes background on prior-data fitted networks, details of the synthetic data generation process, and additional details of the experimental results. The code used in this paper is available at <https://github.com/gmum/zeus>

2 Pre-training representation for clustering

In this section, we introduce our approach to zero-shot representation pre-training for clustering. First, we characterize the proposed probabilistic model and its training objective. Then, we explain the process of generating synthetic datasets for pre-training. Finally, we highlight the connection between our model, Bayesian learning and the framework for prior-data fitted networks.

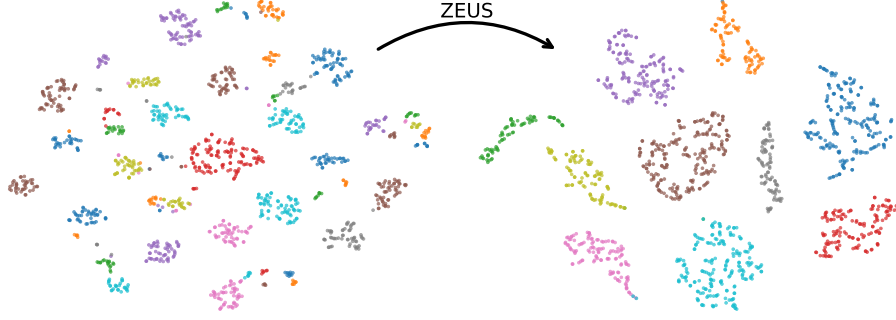


Figure 2: t-SNE visualization for a sample synthetic dataset. The representation from ZEUS (right panel) significantly improves consistency with ground-truth classes and reveals a clearer data structure.

2.1 ZEUS method

Zero-shot pre-training. Traditional machine learning models f_θ are trained by optimizing parameters θ to solve a specific *fixed* task, such as classification or clustering, over a fixed dataset. On the other hand, *in-context learning* (ICL) [8, 19, 13] enables *pre-trained models* f_{θ^*} to adapt to new tasks or datasets without ever updating the pre-trained parameters θ^* . Similarly, *zero-shot learning* allows models to address problems they were never explicitly trained on, without requiring any examples of the target task. Unlike ICL, which adapts through demonstration examples, zero-shot approaches rely entirely on knowledge encoded during pre-training. The pre-training of zero-shot models typically involves massive and diverse datasets that encourage the model to learn rich, generalizable representations of underlying patterns and relationships. This usually is done using *transformers*, as they both can process set-valued inputs (e.g., accept a whole dataset at once) and model complex dependencies.

Our approach involves pre-training a transformer f_θ on a diverse collection of datasets \mathcal{D} such that $\mathcal{D} := (\mathbf{x}, \mathbf{y})$, where $\mathbf{y} = \{y_i\}$ denotes ground-truth labels (e.g., clusters) and $\mathbf{x} = \{x_i\}$ are feature vectors. A loss \mathcal{L} encourages f_θ to assign accurate labels \mathbf{y} to all data points in the target datasets \mathcal{D} :

$$\theta^* = \arg \min_{\theta} \mathbb{E}_{p(\mathcal{D})} [\mathcal{L}(\mathbf{y}, f_\theta(\mathbf{x}))] \approx \arg \min_{\theta} \frac{1}{N_{\mathcal{D}}} \sum_{\mathcal{D} \sim p(\mathcal{D})} \mathcal{L}(\mathbf{y}, f_\theta(\mathbf{x})), \quad (1)$$

where $p(\mathcal{D})$ is a process generating *prior datasets* which *implicitly* characterize a space of possible target tasks (here approximated with $N_{\mathcal{D}}$ Monte-Carlo samples). Note, the loss \mathcal{L} *may factorize* over individual points as $\mathcal{L}(\mathbf{y}, \hat{\mathbf{p}}) = \sum_i \ell(y_i, \hat{p}_i)$, where \hat{p}_i denotes a probabilistic prediction for an individual input x_i , but unlike for classification, for tasks such as clustering or anomaly detection, the predictions $\hat{\mathbf{p}}$ must be made *jointly* for all inputs. Hence, $f_\theta(\mathbf{x})$ can not be decomposed into predictions for individual inputs x_i . Furthermore, in contrast to typical supervised ICL, training labels are not included in the context, as they are unavailable during inference. This makes the unsupervised learning problem significantly more challenging, since we cannot explicitly guide the model toward the desired structure in a given dataset.

Representation learning for probabilistic clustering. We pre-train an encoder f_θ to map inputs \mathbf{x} to representation vectors $z(x_i) = f_\theta(\mathbf{x})_i \in \mathbb{R}^D =: S$. We aim at positioning data points in S , so that they naturally form probabilistic clusters, and our goal is to make the encoder *find better representations for target tasks*. This objective we frame as maximizing the log-likelihood of correct cluster assignments. Since the ground-truth cluster assignments y_i are available during pre-training, this is expressed as:

$$\mathcal{L}_{prob} = - \sum_i \log p_{y_i}(x_i). \quad (2)$$

For specifying $p_y(x)$ we draw an inspiration from Gaussian Mixture Models (GMMs) [5, 14], where each cluster k is represented by a Gaussian distribution centered at c_k , and data points are probabilistically assigned to clusters through probabilities $p_k(x_i)$, based on their proximity to these centroids. Consequently, alongside the encoded representations, we need to define a set of K cluster centroids (e.g., prototypical representations) $\{c_k\}_{k=1}^K$, which reside in the same representation space

S . We then *jointly* optimize \mathcal{L} w.r.t θ and $\{c_k\}$ such that the representations $z(x_i)$ become structured in a way undisclosing *underlying probabilistic structures* in datasets.

We aim at higher probabilities p for points closer these centroids. To achieve this, we first define scores $\alpha_k(x_i) = -\|z(x_i) - c_k\|^2$ to quantify the compatibility between representations and centroids c_k , and then transform them into cluster membership probabilities using softmax, yielding *soft* cluster assignments $p_k(x_i) = \frac{\exp(\alpha_k(x_i))}{\sum_{j=1}^K \exp(\alpha_j(x_i))}$. Note that the ground-truth cluster assignments y_i are known during pre-training, and hence, the maximum likelihood centroids can be straightforward estimated as $\hat{c}_k = \frac{1}{N_k} \sum_{\{i: y_i=k\}} z(x_i)$, where N_k denotes the number of data points assigned to the k -th cluster. Following this formulation, the optimization needs to be performed only w.r.t the parameters θ of the neural network f_θ , as the centroids are already specified by them.

Besides the centroids, we additionally consider another concept from GMMs, namely cluster priors π_k . Similar to centroids, the prior cluster frequencies $\hat{\pi}_k$ can be estimated from the training labels as the proportions of examples in the k -th cluster, and then incorporated directly into the probability calculation, resulting in the final form of our probabilistic scoring:

$$p_k(x_i) = \frac{\hat{\pi}_k \exp(\alpha_k(x_i))}{\sum_{j=1}^K \hat{\pi}_j \exp(\alpha_j(x_i))}, \quad \text{where} \quad \alpha_k(x_i) = -\|z(x_i) - \hat{c}_k\|^2. \quad (3)$$

Remark 2.1. *ZEUS cluster assignments correspond to the membership probabilities in GMMs defined as: $r_{ik} = \frac{\pi_k \mathcal{N}(z(x_i)|c_k, \Sigma_k)}{\sum_{j=1}^K \pi_j \mathcal{N}(z(x_i)|c_j, \Sigma_j)}$, but with fixed diagonal covariance matrices $\Sigma_k := I$, effectively forcing the encoder to learn circular clusters rather than elliptical ones.*

Inference. The structural relations learned during pre-training are leveraged during inference when the representations z produced by the model f_{θ^*} are used to create a predictive distribution for new, previously unseen inputs \mathbf{x}^* as $\hat{\mathbf{p}}^* := p(\mathbf{y}^* | f_{\theta^*}(\mathbf{x}^*))$. At this point, the labels \mathbf{y}^* are unknown and therefore, cannot be used to estimate the centroids nor the priors. Hence, to structure the obtained representation into clusters, we use a traditional learning algorithm, for example, similar to GMMs relying on Expectation-Maximization or simply k-means.

Regularization. Although theoretically \mathcal{L}_{prob} is sufficient to build a clustering representation, we experimentally verified that the introducing additional regularizers further improves the predictions in the inference (see Section 3.4).

First, we aim to ensure that the representations $z(x_i)$ associated with a particular cluster are compactly distributed around their corresponding centroid to enhance intra-cluster cohesion. A point concentration regularizer that explicitly minimizes the distance between representations and the centroids, analogous to the k-means objective of minimizing within-cluster sum of squares, we define as

$$\mathcal{L}_{cp} = \sum_k \sum_{i: y_i=k} \alpha_k(x_i). \quad (4)$$

Second, to prevent the cluster centroids c_k from collapsing towards similar points in the space, we add a centroid separation regularizer. We achieve this by maximizing the sum of squared distances between all distinct pairs of centroids. However, to avoid this term dominating the loss if centroids were pushed infinitely far apart, we cap the contribution of each pair's squared distance at a predefined threshold T . The term to be minimized is thus:

$$\mathcal{L}_{sep} = - \sum_{k=1}^K \sum_{j=k+1}^K \min(\|\hat{c}_k - \hat{c}_j\|^2, T). \quad (5)$$

The *final loss* combines the main clustering objective with two regularization terms as

$$\mathcal{L} = \mathcal{L}_{prob} + \lambda_{cp} \mathcal{L}_{cp} + \lambda_{sep} \mathcal{L}_{sep} \quad (6)$$

where the hyperparameters $\lambda_{cp} \geq 0$ and $\lambda_{sep} \geq 0$ promote point concentration and control the relative importance of enforcing centroid separation, respectively. We used simply $\lambda_{cp} = \lambda_{sep} = 1$.

2.2 Prior data for pre-training ZEUS

The key component of ZEUS is the data-generating prior $p(\mathcal{D})$. As it primarily affects the generalization ability of the pre-trained model f_{θ^*} , it must be designed to cover diverse data distributions and various cluster configurations. In particular, we construct it as a latent variable model (LVM), assuming that each dataset \mathcal{D} is sampled from a K -component mixture of distributions. Formally, the probability of a data point $x \in \mathcal{D}$ under this model is $p(x) = \sum_{k=1}^K p(y = k) p(x | y = k)$, where $p(y)$ is a categorical distribution, and $p(x | y = k)$ represents the k -th (continuous) component. Although the categories y remain latent for real datasets, they are known during synthetic data generation and can serve as ground-truth labels – a property integral to pre-training ZEUS.

The number of categories K we sample uniformly between 2 and 10, and the observations x are sampled from multivariate Gaussian distributions. To control the complexity of datasets, we introduce a constraint that provides a sufficient separation between each pair of components. For each component, we generate between 50 and 800 samples. Since real data rarely consist of Gaussian clusters, we additionally transform the data points from each category using randomized ResNet-like neural networks to produce more realistic cluster shapes. We selected ResNets due to their properties, as they can define invertible transformations [1], and this ensures that clustering structures will be preserved in outputs. Finally, we append a certain fraction of categorical features in one-hot encoding scheme to selected datasets, which is followed by an optional PCA reduction to keep the data dimension at the requested maximum level. Complete details of the prior-data generating process can be found in Appendix B.

The above strategy for generating clustering datasets illustrates the key idea behind ZEUS. Instead of clustering each dataset individually using an arbitrary loss criterion (as in k -means or DEC), ZEUS learns to perform clustering by inverting the data generation process. Although our synthetic datasets are limited by the selected family of distributions specified above, the proposed paradigm for zero-shot unsupervised learning for clustering is general.

2.3 Relation to Bayesian learning and Prior-Data Fitted Networks

The recently introduced framework of *Bayesian inference through transformers* demonstrates that neural networks pre-trained on synthetic datasets implicitly approximate Bayesian inference without explicitly computing posterior distributions [23, 15]. By framing the approach described in Section 2.1 as a Prior-Data Fitted Network (PFN), we show ZEUS implicitly performs approximate Bayesian averaging.

Given a distribution $p(\mathcal{D})$ over (synthetic) datasets \mathcal{D} , a PFN parameterized by θ is trained to minimize the negative log-likelihood of predicting held-out labels within datasets sampled from this prior. The associated loss function is defined as: $\mathcal{L}_{PFN}(\theta) = \mathbb{E}_{\mathcal{D}_{ctx} \cup \{(x,y)\} \sim p(\mathcal{D})} [-\log q_{\theta}(y|x, \mathcal{D}_{ctx})]$. Minimizing the Prior-Data Negative Log-Likelihood is then equivalent to minimizing the expected Kullback–Leibler divergence between the network’s predictive distribution and the true Posterior Predictive Distribution (PPD) $p(y|x, \mathcal{D}_{ctx}) = \int_{\Phi} p(y|x, \phi) p(\mathcal{D}_{ctx}|\phi) p(\phi) d\phi$ (see Corollary 1.1 in [23]). A pre-trained PFN approximates this integral implicitly, yielding a distribution $q_{\theta}(y|x, \mathcal{D}_{ctx})$ directly from forward propagation of the network. In Appendix A, a more detailed explanation of PFNs was provided.

ZEUS instead of directly outputting $q_{\theta}(y|x, \mathcal{D}_{ctx})$, maps inputs x to latent representation vectors $z(x)$. The probabilistic assignments $p_y(x)$ are then constructed from these vectors according to Eq. 3. This equation specifies a PPD for inference, but also defines a probability mass function for training:

Remark 2.2. *Eqs. 1, 2, and 3 constitute a valid Prior-Data Negative Log-Likelihood, equivalent to Eq. (2) from [23] with $\mathcal{D}_{ctx} = \emptyset$.*

This follows by mapping $p_y(x) := q_{\theta}(y|x, \emptyset)$ and noting that Eq. 2 corresponds to the cross-entropy between the true labels $\{y\}$ and the probabilistic assignments $p_y(x)$. Intuitively, this formulation reinterprets probabilistic clustering with known labels as a classification task. Then, pre-training the transformer by minimizing the cross-entropy loss over prior-generated datasets remains identical to PFNs, and thus, we can conclude that ZEUS *implicitly learns a Bayesian approximation through prior fitting*.

Our method, however, deviates from traditional PFNs by imposing an explicit mixture-like structure on latent representations (Eq. 3), unlike more general PFNs:

Remark 2.3. *By enforcing the clustering structure, ZEUS may impose stronger assumptions on the PPD compared to vanilla PFNs. This structure might be suboptimal for classification tasks and the true PPD may not belong to the family of attainable solutions.*

As explained above our clustering-based extension is theoretically sound, nonetheless, the assumption could limit representational expressivity compared to the more flexible transformers employed for the original PFNs [15]. On the other hand, the enforced structures shall be more appropriate for unsupervised tasks.

3 Experiments

This section provides an experimental evaluation of the clustering performance of our method.

3.1 Experimental setup

Model architecture: ZEUS relies on a transformer architecture similar to TabPFN [15]. It consists of 12 attention blocks, each with 6 heads and a token dimension of 512, employing GeLU as the activation function. Following the TabPFN approach, each data point is linearly embedded prior to the transformer component and then treated as a token.

Pre-training: In the pre-training phase, we sample datasets from the mixture of Gaussians and transformed mixtures in equal proportions (1:1), generating 1000 unique dataset batch samples for each epoch. For training, we employ the Adam optimizer along with a cosine learning rate scheduler with warm-up, using a learning rate of $2e-5$. The plot illustrating model improvements during the pre-training process is available in Appendix C.

Inference: During inference, preprocessing of each dataset involves standardizing numerical features, followed by scaling them to the range $[-1, 1]$, whereas categorical features are transformed using one-hot encoding. The input size of our model is fixed to 30. For datasets with lower dimensionality, we pad the missing positions with zeros, while for higher-dimensional datasets, we reduce the number of input features via Principal Component Analysis (PCA). Unless stated otherwise, at inference we use k-means applied to the normalized (=scaled to $[-1, 1]$) transformer output in order to obtain clusters from our learned representation.

Datasets: For evaluation, we consider three groups of datasets: real datasets from OpenML (*Real*), synthetic mixtures of Gaussians (*Syn. Gauss.*), and synthetic mixtures of Gaussians transformed by ResNet-like neural networks (*Syn. Transf.*). Both types of synthetic datasets are augmented with categorical variables. The process of generating synthetic datasets is described in Section 2.2.

Each dataset contains at most 2000 samples as per model design and due to memory limitations. The study covers 34 real datasets, selected based on their clustering feasibility, defined as $ARI \geq 0.4$ achieved by at least one of the methods. Additionally, 20 synthetic datasets of each type were generated from the same prior as in the pre-training phase, but with a different random seed to ensure a fair comparison. Detailed statistics of the datasets, such as the number of numerical and categorical features, are provided in Appendix D.

Baselines: We compare ZEUS against a wide spectrum of state-of-the-art clustering methods used for tabular data. It includes k -means (KM), Gaussian Mixture Model (GMM), and deep-learning methods based on autoencoder (AE) architectures, including DEC [29], IDEC [12], and G-CEALS [25]. We additionally consider also k -means and GMM applied in the autoencoder latent space (respectively referred to as AE-KM and AE-GMM) to compare the clustering quality of our representation against the one obtained from the autoencoder.

For AE-based baselines, we employ the standard configuration used in the prior literature, i.e., an architecture comprising of hidden layers with sizes [500, 500, 2000]. We used the latent dimension of 20, which we verified experimentally as the best value. Further details on the hyperparameters and code repositories for the baselines are provided in Appendix E.

Table 1: Clustering quality (ARI) of ZEUS versus competing methods (higher is better).

	KM	GMM	AE-KM	AE-GMM	DEC	IDEC	G-CEALS	ZEUS
Real	55.54	48.49	51.43	53.56	<u>55.93</u>	54.57	40.37	57.43
Syn. Gauss.	89.90	76.93	81.26	81.40	<u>89.36</u>	82.57	62.84	89.03
Syn. Transf.	75.04	75.88	60.45	71.29	<u>79.94</u>	61.26	49.17	86.33

Table 2: Average rank of the methods used in the benchmark (lower is better).

	KM	GMM	AE-KM	AE-GMM	DEC	IDEC	G-CEALS	ZEUS
Real	<u>3.90</u>	4.57	4.72	4.29	3.96	4.31	6.65	3.60
Syn. Gauss.	2.60	3.35	5.40	5.45	3.10	5.50	7.70	<u>2.90</u>
Syn. Transf.	4.45	3.20	6.20	4.25	<u>3.00</u>	5.70	7.05	2.15

Reporting: In the main text, we report only the results aggregated for each group of datasets (*Real*, *Syn. Gauss.*, *Syn. Transf.*), while detailed results for individual datasets can be found in Appendix F. For the reader’s convenience, we **bold** the best results and underline the second-best ones.

3.2 How effective is ZEUS for clustering?

To evaluate performance of the clustering methods, we employ a standard evaluation procedure, where clusters identified by models are expected to correspond to undisclosed ground-truth classes. We use the Adjusted Rand Index (ARI) for quantitative evaluation, and to improve readability, we scale the ARI values by a factor of 100, where 100 indicates perfect clustering and values near 0 represent random grouping. Table 1 presents a summary of ARI scores averaged over 5 random seeds and all datasets within each dataset group. Additionally, Table 2 displays the average rankings for each of the methods.

We observe that ZEUS achieves competitive performance for all three groups of datasets. In particular, it achieves the best average ARI and the best rank for both the OpenML and Synthetic Transformed datasets, e.g., for the most challenging clustering scenarios. Notably, ZEUS outperforms the second-best method, DEC, by more than 6 percentage points, and the classical baselines by over 10 percentage points on the Synthetic Transformed datasets. The results on the Real datasets further demonstrate that ZEUS effectively generalizes the knowledge acquired during the pre-training stage on synthetic data to general data distributions. For the simplest Gaussian datasets, ZEUS ends up in top-3, with results only slightly below those of k-means and DEC. In terms of average rank it gets the second place.

Among the AE-based methods, DEC performs the best, while G-CEALS consistently demonstrates the weakest performance across all datasets. K-means and GMM, as representatives of the classical methods, perform reasonably well. In particular, k-means consistently lands among the best performing methods, which justifies its broad adoption among practitioners, despite being one of the most basic approaches. The detailed results including scores for individuals datasets corresponding to the averages in Tables 1 and 2 can be found in Appendix F.1

Finally, Figure 3 illustrates how the examined clustering methods scale with the increasing number of input data points. ZEUS maintains almost constant time while being only slightly slower than the basic k-means. It shows that the overhead from creating the representations by ZEUS is minimal. On the other hand, the remaining deep clustering algorithms require significantly more time and scale poorly with the increasing input size.

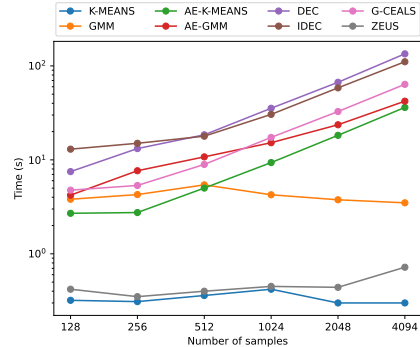


Figure 3: Clustering time vs. input size.

Table 3: Soft clustering quality of ZEUS vs. baselines, measured by Brier score (lower is better).

	KM	GMM	AE-KM	AE-GMM	DEC	IDEC	G-CEALS	ZEUS
Real	0.4366	0.4799	0.4643	0.4679	0.3941	0.3671	0.4722	0.3817
Syn. Gauss.	0.0970	0.3110	0.2073	0.2484	0.3943	0.2308	0.3946	0.1269
Syn. Transf.	0.2803	<u>0.2566</u>	0.4535	0.3140	0.4638	0.3892	0.4951	0.1796

3.3 Are ZEUS’s predictions calibrated?

For applications where uncertainty quantification is as crucial as the clustering decisions themselves, assessing calibration is particularly relevant. Having demonstrated the strong performance of ZEUS for hard clustering, we now examine whether its probabilistic foundations yield well-calibrated soft assignments. We compare it against competing approaches using the Brier score, which measures the accuracy of predicted probabilities. Unlike the previously used ARI, it penalizes both incorrect cluster assignments and *poorly calibrated confidence scores*, thereby providing a more comprehensive evaluation.

The Brier score is a supervised metric, meaning its direct computation for unsupervised clustering tasks is not straightforward. However, when ground-truth classes are available and the number of clusters matches the number of classes, a one-to-one mapping between clusters and classes can be established using the Hungarian algorithm [17, 18], which aims to maximize the total agreement between cluster-class pairs. The cost matrix A for this assignment problem is $A_{jc} = \sum_{i=1}^N p_{ij} \cdot Y_{ic}$, where $Y_{ic} = 1$ if data point i belongs to class c , and $Y_{ic} = 0$ otherwise.

Table 3 reports the average Brier score computed over 5 seeds for all datasets in respective groups. For the analysis, we used the vanilla variant of ZEUS without regularization, which is paired with the GMM clustering since k-means does not provide soft assignments. The covariances were constrained to be identities as implied by Eq. 3. All competing baselines, except for k-means, provide probabilistic cluster assignments, making the Brier score calculation straightforward for them. For k-means, we used one-hot encoding to represent its assignments as probabilities.

ZEUS demonstrates outstanding performance, achieving the best results for the Synthetic Transformed datasets while ranking second on both the OpenML and Synthetic Gaussian collections. The benefits of using ZEUS representations are especially visible in comparison against the vanilla GMM. Although the GMM achieves the second-best score on transformed data, its performance across the remaining datasets is merely modest. Among the remaining baselines, IDEC exhibits an interesting pattern: despite relatively weak clustering performance in Table 1, it achieves the top position on real datasets according to the Brier score and shows marked improvement on synthetic data. DEC displays the opposite tendency, with calibration results significantly inferior to its strong ARI performance. While G-CEALS remains generally weaker than other methods, its calibration performance consistently exceeds its clustering results presented in Table 1. The K-means algorithm, both in its standard implementation and when applied to autoencoder embeddings, yields impressive scores on Gaussian-categorical mixture datasets – likely due to the inherent separability of these data structures, which allows even simple one-hot probability estimates to produce well-calibrated predictions.

3.4 How helpful is regularization for ZEUS?

Representations obtained by minimizing the basic loss \mathcal{L}_{prob} can be further improved by regularizing the optimization process to structure the latent representations. In Table 4, we examine how different combinations of the \mathcal{L}_{prob} loss with the regularizers \mathcal{L}_{cp} and \mathcal{L}_{sep} affect the final performance across various datasets. To ensure a fair comparison, all models were evaluated using a data generator with fixed (identical for all) settings.

Our main model, which during pre-training incorporates both regularizers, exhibits a clear performance advantage on real datasets and consistently holds second place for the synthetic ones. Table 4 shows that a model pre-trained using only \mathcal{L}_{prob} and its variant with \mathcal{L}_{sep} included are insufficient for properly separating the transformer’s representations for the clustering task, as they both struggle with clustering the synthetic datasets encountered during pre-training. On the other hand, the results for $\mathcal{L}_{prob} + \mathcal{L}_{cp}$ imply a positive impact by the compact loss component, \mathcal{L}_{cp} , especially for synthetic

Table 4: Regularisation impact, measured by ARI (higher is better).

	\mathcal{L}_{prob}	$\mathcal{L}_{prob} + \mathcal{L}_{sep}$	$\mathcal{L}_{prob} + \mathcal{L}_{cp}$	$\mathcal{L}_{prob} + \mathcal{L}_{sep} + \mathcal{L}_{cp}$
Real	44.80	<u>51.60</u>	48.65	57.43
Syn. Gauss.	83.37	81.88	90.59	<u>89.03</u>
Syn. Transf.	79.85	79.29	88.58	<u>86.33</u>

data, which however does not translate to strong performance on the OpenML benchmark. We conclude that all three loss components are necessary for good performance, with \mathcal{L}_{cp} being crucial for pre-training and \mathcal{L}_{sep} important for real data.

This mismatch between performance on real and synthetic datasets suggests a potential prior misspecification, which is then mitigated by the regularizers. In particular, among the real datasets, there may be some that are not well explained by the data generation process used during pre-training. Hence, for future work, one may want to explore alternative data-generating priors that may be more appropriate for these outliers.

4 Related work

Tabular data clustering. Traditional clustering algorithms, like k-means [21], GMM [5], or hierarchical methods [24], have widespread applications across data mining, bioinformatics, customer segmentation, and anomaly detection. However, these methods often rely on predefined distance metrics and fail to capture complex, non-linear relationships, making them suboptimal for high-dimensional and heterogeneous tabular datasets.

A pioneering Deep Embedded Clustering (DEC) [29] improves the target data representation by training the autoencoder and computing soft assignments in its latent space via Student’s t -distribution. In a concurrent work [30], the authors perform joint dimensionality reduction using AE and k-means clustering in the latent space of AE. Improved DEC (IDEC) [12] extends DEC by jointly optimizing reconstruction and clustering objectives, while spectral variations replace k-means steps with graph-based updates [7]. G-CEALS [25] replaces the t -distribution assumption with multivariate Gaussian clusters. To eliminate the assumption of explicit distribution prior, DEPICT [6] attaches a softmax layer on top of an embedding network and train with cross-entropy loss. Finally, IDC [28] predicts interpretable cluster assignments at the instance and cluster levels.

However, most of these deep learning models require careful hyperparameter tuning and early stopping which is unrealistic in the fully unsupervised setting due to the lack of labels [26, 27]. Moreover, the optimization process has to be performed on each dataset, which is often time-consuming. Although multiple deep clustering approaches are currently in use, most of them are designed for texts or images [34, 3, 20] and cannot be directly adapted to tabular data due to the lack of a dominant neural architecture for heterogeneous tabular inputs [11, 22].

Representation learning for tabular data. Self-supervised learning (SSL) has been transformative in domains like vision and language [4, 10] but has struggled to show similar success in tabular data [31, 33]. Large diversity of data and lack of pre-defined correlation between features prevents from designing universal pretext tasks or augmentations as well as transferability between domains [32]. In-context learning seems to be a promising direction in representation learning, which enables a single pre-trained model to adapt to new tasks in a zero-shot setting [2]. TabPFN treats small tabular datasets as contexts of (features, labels) and achieves state-of-the-art classification in one forward pass [15]. Although theoretical analyses reveal that transformers can implicitly implement algorithms such as gradient descent *in context*, their use is currently restricted to supervised problems [9].

5 Conclusion

In this paper, we presented ZEUS, a zero-shot transformer-based model that enables effective and efficient clustering of tabular data without the need for fine-tuning or extensive hyperparameter search. By pre-training on synthetic datasets with known latent structures, ZEUS learns generalizable representations that help simple clustering algorithms to uncover meaningful structures. Our experi-

ments show that ZEUS consistently matches or outperforms both classical and deep learning-based clustering methods, offering a practical and theoretically grounded solution for unsupervised analysis of tabular data.

Limitations. Since ZEUS is technically based on the TabPFN architecture, it inherits some of its drawbacks: a maximum number of input features and samples. However, the recently introduced TabPFN v2 [16] showed that tabular transformers can process larger datasets with a negligible increase in computational time. Moreover, our experimental results demonstrate that even if the dimension of input data exceeds the fixed value of 30, applying PCA does not significantly hurt the clustering performance.

The final performance of ZEUS heavily relies on the synthetic data used in pre-training. While we release a basic version of ZEUS, which encodes certain assumptions about data clusters, one can adjust the pre-training stage using different datasets. Finally, ZEUS does not cluster data itself, but constructs a convenient embedding space in which clustering can be performed using basic algorithms.

Acknowledgments and Disclosure of Funding

This research is part of the project No. 2022/45/P/ST6/02969 co-funded by the National Science Centre and the European Union Framework Programme for Research and Innovation Horizon 2020 under the Marie Skłodowska-Curie grant agreement No. 945339.

For the purpose of Open Access, the authors have applied a CC-BY public copyright licence to any Author Accepted Manuscript (AAM) version arising from this submission.



The research of M. Śmieja and P. Marszałek was supported by the National Science Centre (Poland), grant no. 2023/50/E/ST6/00169.

The research of J. Tabor was supported by the National Science Centre (Poland), grant no. 2023/49/B/ST6/01137.

Witold Wydmański is supported by the Ministry of Science grant no. PN/01/0195/2022 and NCN Sonata BIS grant number 2020/38/E/NZ2/00598.

References

- [1] J. Behrmann, W. Grathwohl, R. T. Q. Chen, D. Duvenaud, and J.-H. Jacobsen. Invertible residual networks, 2019.
- [2] T. B. Brown, B. Mann, N. Ryder, M. Subbiah, J. Kaplan, P. Dhariwal, A. Neelakantan, P. Shyam, G. Sastry, A. Askell, S. Agarwal, A. Herbert-Voss, G. Krueger, T. Henighan, R. Child, A. Ramesh, D. M. Ziegler, J. Wu, C. Winter, C. Hesse, M. Chen, E. Sigler, M. Litwin, S. Gray, B. Chess, J. Clark, C. Berner, S. McCandlish, A. Radford, I. Sutskever, and D. Amodei. Language models are few-shot learners, 2020.
- [3] S. Cai, L. Qiu, X. Chen, Q. Zhang, and L. Chen. Semantic-enhanced image clustering. In *Proceedings of the AAAI conference on artificial intelligence*, volume 37, pages 6869–6878, 2023.
- [4] T. Chen, S. Kornblith, M. Norouzi, and G. Hinton. A simple framework for contrastive learning of visual representations. In *International conference on machine learning*, pages 1597–1607. PmLR, 2020.
- [5] A. P. Dempster, N. M. Laird, and D. B. Rubin. Maximum likelihood from incomplete data via the em algorithm. *Journal of the royal statistical society: series B (methodological)*, 39(1):1–22, 1977.
- [6] K. G. Dizaji, A. Herandi, C. Deng, W. Cai, and H. Huang. Deep clustering via joint convolutional autoencoder embedding and relative entropy minimization, 2017.

- [7] L. Duan, C. Aggarwal, S. Ma, and S. Sathe. Improving spectral clustering with deep embedding and cluster estimation. In *2019 IEEE International Conference on Data Mining (ICDM)*, pages 170–179, 2019.
- [8] S. Garg, D. Tsipras, P. Liang, and G. Valiant. What can transformers learn in-context? a case study of simple function classes. In *Proceedings of the 36th International Conference on Neural Information Processing Systems, NIPS ’22*, Red Hook, NY, USA, 2022. Curran Associates Inc.
- [9] S. Garg, D. Tsipras, P. Liang, and G. Valiant. What can transformers learn in-context? a case study of simple function classes, 2023.
- [10] J.-B. Grill, F. Strub, F. Altché, C. Tallec, P. Richemond, E. Buchatskaya, C. Doersch, B. Avila Pires, Z. Guo, M. Gheshlaghi Azar, et al. Bootstrap your own latent-a new approach to self-supervised learning. *Advances in neural information processing systems*, 33:21271–21284, 2020.
- [11] L. Grinsztajn, E. Oyallon, and G. Varoquaux. Why do tree-based models still outperform deep learning on tabular data? arxiv. *arXiv preprint arXiv:2207.08815*, 2022.
- [12] X. Guo, L. Gao, X. Liu, and J. Yin. Improved Deep Embedded Clustering with Local Structure Preservation. In *Proceedings of the Twenty-Sixth International Joint Conference on Artificial Intelligence, IJCAI-17*, pages 1753–1759, 2017.
- [13] X. Han, D. Simig, T. Mihaylov, Y. Tsvetkov, A. Celikyilmaz, and T. Wang. Understanding in-context learning via supportive pretraining data. In A. Rogers, J. Boyd-Graber, and N. Okazaki, editors, *Proceedings of the 61st Annual Meeting of the Association for Computational Linguistics (Volume 1: Long Papers)*, pages 12660–12673, Toronto, Canada, July 2023. Association for Computational Linguistics.
- [14] L. P. Hansen. Large sample properties of generalized method of moments estimators. *Econometrica: Journal of the econometric society*, pages 1029–1054, 1982.
- [15] N. Hollmann, S. Müller, K. Eggenberger, and F. Hutter. TabPFN: A transformer that solves small tabular classification problems in a second. In *The Eleventh International Conference on Learning Representations*, 2023.
- [16] N. Hollmann, S. Müller, L. Purucker, A. Krishnakumar, M. Körfer, S. B. Hoo, R. T. Schirrmeister, and F. Hutter. Accurate predictions on small data with a tabular foundation model. *Nature*, 637(8045):319–326, 2025.
- [17] H. W. Kuhn. The hungarian method for the assignment problem. *Naval research logistics quarterly*, 2(1-2):83–97, 1955.
- [18] H. W. Kuhn. Variants of the hungarian method for assignment problems. *Naval research logistics quarterly*, 3(4):253–258, 1956.
- [19] J. Lee, A. Xie, A. Pacchiano, Y. Chandak, C. Finn, O. Nachum, and E. Brunskill. Supervised pretraining can learn in-context reinforcement learning. In *Thirty-seventh Conference on Neural Information Processing Systems*, 2023.
- [20] Y. Li, P. Hu, D. Peng, J. Lv, J. Fan, and X. Peng. Image clustering with external guidance. In *International Conference on Machine Learning*, pages 27890–27902. PMLR, 2024.
- [21] J. MacQueen. Some methods for classification and analysis of multivariate observations. In *Proceedings of the Fifth Berkeley Symposium on Mathematical Statistics and Probability, Volume 1: Statistics*, volume 5, pages 281–298. University of California press, 1967.
- [22] D. McElfresh, S. Khandagale, J. Valverde, V. Prasad C, G. Ramakrishnan, M. Goldblum, and C. White. When do neural nets outperform boosted trees on tabular data? *Advances in Neural Information Processing Systems*, 36:76336–76369, 2023.
- [23] S. Müller, N. Hollmann, S. P. Arango, J. Grabocka, and F. Hutter. Transformers can do bayesian inference. In *International Conference on Learning Representations*, 2022.

- [24] F. Murtagh and P. Contreras. Algorithms for hierarchical clustering: an overview. *Wiley Interdisciplinary Reviews: Data Mining and Knowledge Discovery*, 2(1):86–97, 2012.
- [25] S. B. Rabbani, I. V. Medri, and M. D. Samad. Deep clustering of tabular data by weighted gaussian distribution learning. *Neurocomputing*, 623:129359, 2025.
- [26] M. Sadeghi and N. Armanfard. Idecf: Improved deep embedding clustering with deep fuzzy supervision. In *2021 IEEE International Conference on Image Processing (ICIP)*, pages 1009–1013, 2021.
- [27] M. Sadeghi and N. Armanfard. Deep clustering with self-supervision using pairwise similarities, 2024.
- [28] J. Svirsky and O. Lindenbaum. Interpretable deep clustering for tabular data. *arXiv preprint arXiv:2306.04785*, 2023.
- [29] J. Xie, R. Girshick, and A. Farhadi. Unsupervised deep embedding for clustering analysis, 2016.
- [30] B. Yang, X. Fu, N. D. Sidiropoulos, and M. Hong. Towards k-means-friendly spaces: Simultaneous deep learning and clustering. In *international conference on machine learning*, pages 3861–3870. PMLR, 2017.
- [31] J. Yoon, Y. Zhang, J. Jordon, and M. Van der Schaar. Vime: Extending the success of self-and semi-supervised learning to tabular domain. *Advances in neural information processing systems*, 33:11033–11043, 2020.
- [32] Z. Zhao, L. Alzubaidi, J. Zhang, Y. Duan, and Y. Gu. A comparison review of transfer learning and self-supervised learning: Definitions, applications, advantages and limitations. *Expert Systems with Applications*, 242:122807, 2024.
- [33] B. Zhu, X. Shi, N. Erickson, M. Li, G. Karypis, and M. Shoaran. Xtab: cross-table pretraining for tabular transformers. In *Proceedings of the 40th International Conference on Machine Learning*, pages 43181–43204, 2023.
- [34] M. Znalezniak, P. Rola, P. Kaszuba, J. Tabor, and M. Śmieja. Contrastive hierarchical clustering. In *Joint European Conference on Machine Learning and Knowledge Discovery in Databases*, pages 627–643. Springer, 2023.

A Background on Prior-Data Fitted Networks

The recently introduced framework of *Bayesian inference through transformers* demonstrates that neural networks pre-trained on synthetic datasets implicitly approximate Bayesian inference without explicitly computing posterior distributions [23, 15]. The pre-trained transformers are known as *Prior-Data Fitted Networks* (PFNs). The pre-training involves synthetic prior fitting, wherein a transformer network is trained offline on numerous datasets generated from a predefined prior distribution over tasks. This pre-training procedure allows the transformer to implicitly encode a Bayesian posterior predictive distribution by optimizing a cross-entropy loss between its predictions and the synthetic data labels.

Formally, pre-training is carried out as follows: given a prior distribution $p(\mathcal{D})$ over (synthetic) datasets \mathcal{D} , a PFN network parameterized by θ is trained to minimize the negative log-likelihood of predicting held-out labels within datasets sampled from this prior. The associated loss function, known as the Prior-Data Negative Log-Likelihood (Prior-Data NLL), is explicitly defined as:

$$\mathcal{L}_{PFN}(\theta) = \mathbb{E}_{\mathcal{D}_{ctx} \cup \{(x,y)\} \sim p(\mathcal{D})} [-\log q_{\theta}(y|x, \mathcal{D}_{ctx})],$$

where each dataset \mathcal{D}_{ctx} and data point (x, y) are sampled from the predefined prior distribution $p(\mathcal{D})$. As shown formally in [23], minimizing this loss is mathematically equivalent to minimizing the expected cross-entropy between the predictive distribution $q_{\theta}(y|x, \mathcal{D}_{ctx})$ and the true posterior predictive distribution (PPD) derived from the prior. Specifically, minimizing the Prior-Data NLL is equivalent to minimizing the expected Kullback–Leibler divergence between the network’s predictive distribution and the true PPD $p(y|x, \mathcal{D}_{ctx})$:

$$\mathcal{L}_{PFN}(\theta) = \mathbb{E}_{\mathcal{D}_{ctx}, x \sim p(\mathcal{D})} [H(p(\cdot|x, \mathcal{D}), q_{\theta}(\cdot|x, \mathcal{D}_{ctx}))],$$

where H denotes the cross-entropy. Thus, optimality of the predictive distribution q_{θ} implies matching it exactly to the true Bayesian posterior predictive distribution, provided that the parametric family of distributions defined by the transformer is sufficiently expressive [23].

Within this in-context learning as Bayesian inference framework, transformers approximate Bayesian averaging implicitly. Given a training dataset $\mathcal{D}_{ctx} = \{(x_i, y_i)\}_{i=1}^n$, a new input x , and a prior over hypotheses ϕ , the Bayesian posterior predictive distribution is formally expressed as:

$$p(y|x, \mathcal{D}_{ctx}) = \int_{\Phi} p(y|x, \phi) p(\mathcal{D}_{ctx}|\phi) p(\phi) d\phi,$$

integrating over all hypotheses $\phi \in \Phi$. PFNs approximate this integral implicitly through pre-training on prior-generated datasets, yielding a distribution $q_{\theta}(y|x, \mathcal{D}_{ctx})$ directly from forward propagation of the network conditioned on dataset \mathcal{D}_{ctx} [23, 15].

B Details of synthetic data generation process

We use three types of probabilistic models to generate data from a category:

1. **Gaussian.** The continuous features of each cluster follow a multivariate Gaussian distribution with carefully constructed means and covariance matrices. Cluster means are placed with a minimum Wasserstein-2 distance constraint to ensure adequate separation between clusters and to prevent trivial overlap cases. The exact minimum distance value varies between 0.5 and 1.0 and is randomly selected for each component independently in order to promote data diversity. The covariance structure for each Gaussian is generated through eigendecomposition, with eigenvalues sampled from a predefined range of [0.005, 0.05] to control the shape and orientation of the clusters. Additionally, to guarantee the presence of both full-rank Gaussians in higher dimensions and degenerate ones in lower dimensions, extra conditions are introduced to narrow the range of eigenvalues. These constraints are activated with probabilities of 0.25 and 0.2, respectively. The process of constructing Gaussian mixture is incremental. Starting with a mixture containing k components, the addition of a new cluster involves initially placing it at position 0 and then shifting it in a randomly chosen direction until the distance requirement is satisfied. This entire approach allows us to model a variety of cluster geometries, from spherical to highly elongated elliptical shapes.

2. **Categorical.** We also incorporate categorical features alongside continuous ones by sampling from categorical distributions that are biased toward certain categories for each cluster. To generate these varied categorical probability patterns, we use the Dirichlet distribution. The resulting categorical variables are then converted to one-hot encoding and combined with the continuous features, producing mixed-type datasets that more closely resemble real-world tabular data. The probability of including categorical features is controlled by a *categorical_chance* parameter, set to 0.3. Up to 3 categorical variables may be added, each having between 2 and *max_categories* possible values, defined as 5.
3. **NN transformed.** To create more complex, non-linearly separable cluster structures, we apply transformations to the numerical features using random neural networks with 3 to 6 layers. These transformations map the original data through several non-linear operations while preserving cluster identity information, producing datasets with more challenging decision boundaries. Following the approach of Invertible Residual Networks [1], we constrain the spectral norm of each transformation layer to be less than 1. In addition, standardization is applied between residual layers to ensure more stable transformations. To help preserve cluster separability, we append one-hot vectors encoding the component identity of each data point to the numerical variables before passing them through the random neural network. After the transformation, these extra dimensions are removed using PCA, restoring the data to its original dimensionality. This comprehensive approach enables the simulation of intricate, non-linear data manifold structures often presented in real-world clustering problems without introducing degenerate configurations.

Afterwards, all features undergo standardization and scaling to ensure numerical stability during training. Continuous features are normalized to the range $[-1, 1]$, while ensuring that the relative separation between clusters is preserved.

By training on this diverse collection of synthetic datasets-ranging from well-separated Gaussian clusters to complex, transformed manifolds with mixed feature types-our model learns to identify meaningful cluster structures across a wide spectrum of data distributions. This comprehensive prior fitting enables ZEUS to adapt to previously unseen datasets at inference time without additional training.

C Pre-training plots

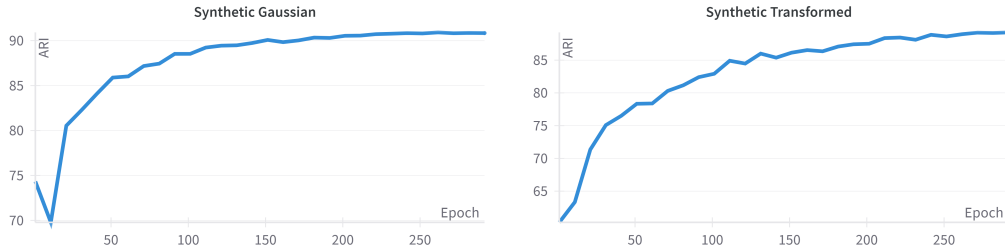


Figure 4: Visualization of pre-training process

Figure 4 presents two plots of average ARI over 200 synthetic validation datasets throughout 300 pre-training epochs. The first plot corresponds to the Gaussian-categorical datasets referred to as Synthetic Gaussian, while the second illustrates their NN transformed variants, named Synthetic Transformed. The data generation procedures are described in more detail in Appendix B. Both plots illustrate that the quality of the ZEUS representation improves over time, indicating that the model is learning new patterns, as evidenced by the increasing ARI during the pre-training process.

D Statistics of datasets used in experimental study

Tables 5, 6, and 7 provide detailed information about the datasets used in the experimental analysis. Each table includes the number of set instances, the number of categorical and numerical features, the

Table 5: Real/OpenML datasets statistics.

ID	# Instances	# Numerical features	# Categorical features	Dimension	# Categories (one-hots)	# Classes
14	2000	76	0	76	0	10
15	699	9	0	9	0	2
16	2000	64	0	64	0	10
18	2000	6	0	6	0	10
22	2000	47	0	47	0	10
35	366	1	33	130	129	6
51	294	6	7	25	19	2
53	270	13	0	13	0	2
56	435	0	16	32	32	2
61	150	4	0	4	0	3
187	178	13	0	13	0	3
377	600	60	0	60	0	6
458	841	70	0	70	0	4
481	209	7	1	14	7	2
694	310	8	0	8	0	9
721	200	10	0	10	0	2
733	209	6	0	6	0	2
745	159	14	1	20	6	2
756	159	15	0	15	0	2
796	209	6	1	36	30	2
820	235	12	0	12	0	2
840	205	17	8	68	51	2
854	158	5	2	14	9	2
1462	1372	4	0	4	0	2
1495	250	0	6	18	18	2
1499	210	7	0	7	0	3
1510	569	30	0	30	0	2
1523	310	6	0	6	0	3
4153	180	66	0	66	0	6
40496	500	7	0	7	0	10
40682	215	5	0	5	0	3
40705	959	42	2	44	2	2
42261	150	4	0	4	0	3
42585	344	4	2	10	6	3

total dimensionality, and the overall number of categories, represented by the length of the one-hot encoded vectors. Additionally, the tables report the number of classes that each dataset contains. In Table 5, the ID column corresponds to the OpenML ID, while in the remaining tables it functions solely as an index.

E Baselines

The evaluation of baseline models is based on the following libraries and GitHub repositories:

1. **scikit-learn** - used for k-means and GMM
2. <https://github.com/vlukiyanov/pt-dec> - implementation of the DEC
3. <https://github.com/dawnranger/IDEC-pytorch> - source code for the IDEC
4. <https://github.com/mdsamad001/G-CEALS—Deep-Clustering-for-Tabular-Data> - code-base for the GCEALS

To ensure fair comparison, hyperparameters are chosen to maximize the performance of each method with respect to their overall average rank across 5 random seeds. For this reason, all numerical features are preprocessed using a standard scaler prior to the training phase.

Table 6: Synthetic gaussian datasets statistics.

ID	# Instances	# Numerical features	# Categorical features	Dimension	# Categories (one-hots)	# Classes
0	1337	16	0	16	0	8
1	1383	23	0	23	0	8
2	1421	8	2	14	6	7
3	992	9	1	12	3	9
4	1314	8	0	8	0	9
5	1497	16	2	23	7	8
6	1370	2	0	2	0	6
7	1646	4	3	16	12	8
8	1520	11	0	11	0	8
9	1537	18	0	18	0	5
10	825	26	0	26	0	2
11	1112	9	0	9	0	5
12	1093	15	0	15	0	8
13	742	6	0	6	0	3
14	1595	11	2	18	7	7
15	1417	14	0	14	0	6
16	1787	28	0	28	0	5
17	764	19	0	19	0	4
18	889	25	0	25	0	5
19	1660	28	0	28	0	9

Table 7: Synthetic transformed datasets statistics.

ID	# Instances	# Numerical features	# Categorical features	Dimension	# Categories (one-hots)	# Classes
0	1337	16	0	16	0	8
1	1627	30	0	30	0	9
2	1631	11	0	11	0	7
3	1891	15	1	17	2	10
4	1142	3	0	3	0	4
5	1222	24	0	24	0	9
6	953	6	0	6	0	6
7	1508	9	0	9	0	10
8	840	7	3	15	8	5
9	1745	14	0	14	0	9
10	1618	23	0	23	0	6
11	1432	13	0	13	0	9
12	1860	9	0	9	0	9
13	563	10	0	10	0	2
14	1033	6	2	13	7	3
15	750	2	0	2	0	4
16	1451	14	2	20	6	10
17	679	30	0	30	0	2
18	859	22	1	25	3	2
19	1493	11	0	11	0	7

Most parameters of the k-means and GMM methods are left at their default values. Only the n_{init} option was increased to 100 for k-means and 50 for GMM in order to improve stability.

As mentioned in Section 3.1, a standard autoencoder with hidden layers [500, 500, 2000] is used for each AE-based method. The resulting network is first pre-trained for 1000 epochs and then fine-tuned for up to 1000 additional epochs, separately for each dataset and model. Following the GCEALS evaluation procedure, multiple latent dimension sizes [5, 10, 15, 20] were tested across all

considered methods. The results indicate that the default latent dimension of 10 does not yield the best performance; instead, a dimension of 20 generally performs better. Changing other hyperparameters, including the learning rate, optimizer, and clustering loss weight γ , generally did not lead to improved results. Therefore, the remaining parameters were left at their default values as proposed by the authors of the respective repositories.

Table 8: Real/OpenML datasets - ARI

ID	KM	GMM	AE-KM	AE-GMM	DEC	IDEC	G-CEALS	ZEUS
14	38.74	45.90	40.94	45.36	<u>49.60</u>	36.78	45.04	50.56
15	82.85	71.38	61.44	71.74	<u>86.29</u>	87.48	24.38	81.28
16	55.62	64.75	61.66	<u>69.97</u>	<u>68.56</u>	55.61	55.27	74.03
18	54.86	46.88	51.45	<u>51.47</u>	50.00	<u>53.54</u>	49.93	51.63
22	35.48	47.39	31.09	<u>50.80</u>	50.02	35.69	28.38	56.05
35	<u>70.68</u>	<u>70.68</u>	70.22	70.48	68.63	64.58	56.57	85.12
51	28.35	-2.54	37.82	34.13	<u>38.13</u>	34.58	35.13	43.66
53	45.21	5.17	39.14	40.62	<u>43.50</u>	41.91	21.32	35.76
56	57.79	<u>58.49</u>	57.10	58.31	<u>56.97</u>	55.20	55.66	66.41
61	62.01	90.39	59.79	60.21	57.84	60.14	51.37	<u>85.15</u>
187	<u>89.75</u>	93.09	82.87	84.86	85.02	85.10	55.67	88.19
377	56.70	58.47	<u>62.06</u>	59.52	63.03	59.01	59.79	55.30
458	95.08	96.97	64.33	75.70	94.58	63.29	68.31	99.19
481	58.51	2.77	36.84	48.03	<u>57.28</u>	52.93	19.67	8.68
694	35.91	43.30	35.26	<u>36.56</u>	<u>26.30</u>	36.02	30.76	33.38
721	43.28	43.28	13.12	<u>25.12</u>	17.75	<u>28.77</u>	-0.03	43.28
733	50.97	46.29	38.39	55.11	67.47	<u>73.51</u>	26.26	74.97
745	57.63	55.44	78.35	<u>75.52</u>	46.37	50.94	57.81	73.85
756	55.70	4.46	72.81	<u>53.40</u>	58.60	<u>65.58</u>	44.14	50.31
796	49.62	2.26	76.54	52.19	50.07	<u>55.92</u>	43.40	13.99
820	<u>50.16</u>	36.77	44.29	49.24	51.21	49.30	24.51	28.87
840	<u>39.05</u>	48.37	53.60	46.72	<u>49.14</u>	39.16	27.95	27.66
854	76.14	-0.21	62.33	60.83	35.05	70.52	<u>72.25</u>	76.14
1462	1.32	0.31	10.03	<u>10.17</u>	1.00	3.80	8.48	92.28
1495	96.81	98.40	72.74	<u>82.80</u>	<u>96.81</u>	91.28	77.51	7.35
1499	77.33	62.99	73.68	75.28	69.99	<u>78.48</u>	29.60	82.40
1510	67.07	78.02	63.73	59.77	71.32	69.84	69.47	<u>74.26</u>
1523	21.16	41.21	25.48	24.57	<u>28.16</u>	23.05	18.50	<u>19.60</u>
4153	55.78	58.03	<u>59.15</u>	46.23	56.41	58.44	39.43	62.29
40496	54.02	34.79	42.35	37.51	<u>49.74</u>	42.35	37.33	32.25
40682	58.32	86.29	57.89	59.22	<u>57.39</u>	<u>86.05</u>	40.58	53.15
40705	43.49	37.92	0.73	30.63	47.90	<u>46.28</u>	10.71	45.45
42261	62.01	90.39	60.13	58.15	59.78	56.78	49.09	<u>85.15</u>
42585	60.84	30.52	51.26	60.71	<u>91.79</u>	43.40	38.30	95.05
Mean	55.54	48.49	51.43	53.56	<u>55.93</u>	54.57	40.37	57.43
Mean-rank	<u>3.90</u>	4.57	4.72	4.29	3.96	4.31	6.65	3.60
Top-3	16	14	9	8	<u>18</u>	13	2	21
Top-1	4	<u>8</u>	4	0	3	1	0	12

F Extended experimental results

This section presents extended tables corresponding to the experiments described in Section 3.

F.1 How effective is ZEUS for clustering?

Tables 8, 9, and 10 contain the complete results for individual datasets from the experiments discussed in Section 3.2 in Tables 1 and 2, as presented in the main text. The reported values represent averages of ARI over 5 random seeds. In addition to the rows presenting outcomes for specific datasets, the tables include summary rows labeled Mean, Mean-Rank, Top-3, and Top-1. These represent, respectively: the average ARI, the average rank computed across all datasets, the number of times a

Table 9: Synthetic gaussian datasets - ARI

ID	KM	GMM	AE-KM	AE-GMM	DEC	IDEC	G-CEALS	ZEUS
0	86.16	82.13	83.44	79.66	87.06	77.26	58.57	87.65
1	88.66	87.36	81.13	79.61	85.84	75.62	54.10	72.04
2	81.30	26.46	71.57	78.04	86.65	78.91	48.59	<u>82.96</u>
3	<u>95.02</u>	36.77	92.03	76.44	92.74	89.81	62.67	95.76
4	<u>90.64</u>	92.97	82.65	77.80	91.61	84.51	69.70	<u>92.85</u>
5	89.83	25.85	86.52	69.06	<u>90.01</u>	88.31	67.70	90.72
6	96.21	98.07	85.99	94.26	94.24	92.39	73.15	<u>97.89</u>
7	<u>92.59</u>	30.52	81.73	79.06	91.35	89.80	58.10	93.60
8	<u>88.29</u>	89.62	81.15	76.53	87.56	78.37	50.30	84.00
9	93.36	98.54	68.58	85.42	91.14	85.29	56.89	<u>94.55</u>
10	79.26	93.32	72.75	<u>90.90</u>	72.54	73.51	48.47	<u>87.32</u>
11	93.60	98.48	90.77	89.11	95.03	92.19	64.24	<u>97.45</u>
12	86.82	77.45	73.64	71.40	<u>86.04</u>	77.93	58.45	<u>86.04</u>
13	<u>96.77</u>	98.07	94.05	90.15	<u>96.11</u>	85.66	78.20	<u>96.17</u>
14	90.73	43.20	79.65	69.09	<u>92.68</u>	77.93	67.84	94.60
15	93.58	<u>96.23</u>	85.74	89.30	<u>94.43</u>	89.41	72.88	96.68
16	94.70	<u>92.45</u>	90.98	89.41	<u>94.53</u>	88.14	85.86	87.19
17	85.26	87.10	62.23	79.52	84.08	75.00	42.55	<u>86.29</u>
18	<u>88.77</u>	94.83	84.47	84.74	87.39	83.46	67.96	83.01
19	<u>86.54</u>	89.11	76.18	78.46	86.06	67.99	70.50	73.85
Mean	89.90	76.93	81.26	81.40	<u>89.36</u>	82.57	62.84	89.03
Mean-Rank	2.60	3.35	5.40	5.45	3.10	5.50	7.70	<u>2.90</u>
Top-3	16	13	0	1	<u>15</u>	0	0	<u>15</u>
Top-1	3	10	0	0	1	0	0	<u>6</u>

Table 10: Synthetic transformed datasets - ARI

ID	KM	GMM	AE-KM	AE-GMM	DEC	IDEC	G-CEALS	ZEUS
0	60.56	<u>79.33</u>	46.31	68.98	76.93	46.35	29.42	87.42
1	<u>93.30</u>	96.55	76.57	83.99	91.29	70.91	73.09	89.40
2	<u>89.76</u>	96.31	57.79	65.99	94.42	66.34	48.34	<u>95.88</u>
3	70.16	50.38	56.23	76.06	83.06	60.09	54.54	<u>80.98</u>
4	44.32	80.63	47.60	44.77	68.39	50.12	49.37	<u>73.66</u>
5	<u>91.49</u>	96.51	74.48	89.11	86.46	77.84	66.47	<u>81.63</u>
6	60.98	<u>81.63</u>	61.97	76.29	75.58	61.89	69.84	87.02
7	76.80	83.98	71.37	77.69	<u>86.56</u>	77.49	56.51	89.57
8	89.77	77.10	85.53	84.42	<u>93.33</u>	92.96	78.87	98.11
9	84.40	98.48	82.64	93.03	97.14	81.02	65.62	<u>97.20</u>
10	82.47	91.91	61.00	86.16	<u>87.58</u>	46.08	39.27	86.42
11	90.77	99.32	81.41	91.18	<u>94.78</u>	88.12	70.29	93.19
12	67.64	91.80	52.87	63.56	85.45	60.61	55.59	<u>87.75</u>
13	<u>85.99</u>	50.80	45.48	35.34	29.04	12.91	32.89	91.60
14	<u>93.52</u>	54.56	15.81	22.79	<u>94.12</u>	38.21	15.10	98.49
15	36.62	30.93	37.71	43.70	<u>42.78</u>	40.65	29.70	28.96
16	95.62	65.11	90.13	94.97	97.47	95.32	<u>98.27</u>	99.01
17	60.54	<u>95.74</u>	56.24	91.71	78.72	59.11	13.29	96.44
18	63.92	17.39	58.47	<u>70.21</u>	54.61	47.93	10.01	79.70
19	62.12	79.06	49.36	<u>65.77</u>	<u>81.07</u>	51.19	26.84	84.13
Mean	75.04	75.88	60.45	71.29	<u>79.94</u>	61.26	49.17	86.33
Mean-Rank	4.45	3.20	6.20	4.25	<u>3.00</u>	5.70	7.05	2.15
Top-3	5	14	0	6	<u>15</u>	2	1	17
Top-1	0	<u>8</u>	0	1	<u>1</u>	0	0	10

given model appears in the top 3, and the total number of wins achieved by each method. It is worth noting that the Top-1 and Top-3 rows indicate clear wins and clear appearances in top-3 positions.

The overall conclusions align with those presented in the primary analysis. One noteworthy point is that ZEUS achieves strong performance in terms of the Top-3 and Top-1 statistics, being outperformed

in this regard only in Table 9, where k-means and GMM score better. Another interesting observation is that GMM struggles with categorical features, which significantly worsens its average scores in Tables 9 and 10.

F.2 Are ZEUS’s assignments well calibrated?

Table 11, 12 and 13 contain detailed extension of Table 3

Table 11: Real/OpenML datasets - Brier

ID	KM	GMM	AE-KM	AE-GMM	DEC	IDEC	G-CEALS	ZEUS
14	0.7660	0.8579	0.8240	0.7144	0.5338	0.6409	0.7993	0.7006
15	<u>0.0858</u>	0.1548	0.2100	0.1791	0.1489	0.0644	0.2003	0.0973
16	0.5012	0.4982	0.4224	0.5372	0.3726	0.5020	0.6099	0.2761
18	<u>0.6060</u>	0.8529	0.7312	0.6961	0.6099	0.5354	0.6855	0.7094
22	<u>0.8316</u>	0.7533	1.0686	0.7684	0.5071	0.6496	0.7201	0.7173
35	0.0710	0.5016	0.4678	0.5711	0.5881	0.3987	0.3836	<u>0.2552</u>
51	0.3741	0.3741	0.3687	0.3844	0.3297	0.3345	0.3997	<u>0.3333</u>
53	0.4074	0.7052	0.3556	0.6285	<u>0.3361</u>	0.2979	0.5234	0.4000
56	0.2391	0.2344	0.2520	0.2703	0.2147	<u>0.2088</u>	0.2517	0.1829
61	0.2267	0.0570	0.3600	0.3796	0.3881	0.3445	0.4167	<u>0.0979</u>
187	0.0899	0.0622	0.1349	0.1146	0.3380	0.0785	0.2518	<u>0.0762</u>
377	0.8633	0.8320	0.6200	0.6275	<u>0.5316</u>	0.5047	0.5739	0.8508
458	0.0285	<u>0.0214</u>	0.5222	0.3407	0.3203	0.3656	0.4104	0.0048
481	0.8038	0.8134	0.4536	0.2136	0.3111	<u>0.2146</u>	0.4422	0.6986
694	1.0155	0.8831	0.9858	0.9342	0.7616	<u>0.7525</u>	0.7038	0.7621
721	0.3400	0.3400	0.6620	0.6031	0.4491	<u>0.4359</u>	0.7937	0.3400
733	0.1722	0.2859	0.3082	0.4937	0.2115	0.1129	0.3195	<u>0.1244</u>
745	0.2516	0.2516	0.1359	0.2766	0.3016	0.1793	0.2388	<u>0.1384</u>
756	0.2767	0.3615	<u>0.2113</u>	0.3262	0.3178	0.1329	0.4134	0.2767
796	0.0574	0.7943	<u>0.1340</u>	0.3088	0.2046	0.3002	0.5269	0.6253
820	0.2979	0.3720	0.3557	0.2876	0.2334	<u>0.2594</u>	0.3981	0.4596
840	0.8780	0.2790	0.2868	<u>0.2625</u>	0.2746	0.2445	0.4642	0.4665
854	0.6329	0.8203	0.3468	0.4481	0.4469	<u>0.3372</u>	0.3678	0.1266
1462	0.8484	0.8978	0.7688	0.8310	<u>0.6674</u>	0.7714	0.6747	0.0394
1495	<u>0.0160</u>	0.0080	0.1696	0.0397	0.2667	0.0713	0.1583	0.7200
1499	0.2190	0.2933	0.1867	0.1961	0.3939	<u>0.1376</u>	0.4063	0.1239
1510	0.1441	0.1161	0.2257	0.1954	0.2195	0.1432	0.2060	<u>0.1371</u>
1523	1.0516	0.7284	0.9019	0.9708	0.6099	0.7782	<u>0.6316</u>	1.0002
4153	<u>0.7778</u>	0.7178	0.6311	0.8111	<u>0.5757</u>	0.6377	<u>0.8360</u>	0.4651
40496	0.5064	0.9563	0.8312	0.8432	0.6733	<u>0.6143</u>	0.7376	1.0124
40682	0.2233	<u>0.0747</u>	0.2456	0.2251	0.2694	0.0685	0.3210	0.2884
40705	0.3879	<u>0.3837</u>	0.7095	0.4415	0.2541	0.3347	0.4304	<u>0.3254</u>
42261	0.2267	0.0570	0.3413	0.3760	0.3889	0.2854	0.3800	<u>0.1081</u>
42585	0.6279	0.9790	0.5558	0.6111	<u>0.3494</u>	0.7425	0.3795	0.0383
Mean	0.4366	0.4799	0.4643	0.4679	0.3941	0.3671	0.4722	<u>0.3817</u>
Mean-Rank	4.54	4.94	5.12	5.50	3.88	2.85	5.65	<u>3.51</u>
Top-3	12	9	8	4	19	22	6	<u>21</u>
Top-1	3	5	1	1	<u>6</u>	8	1	8

F.3 How helpful is regularization for ZEUS?

Tables 14, 15 and 16 provide extended versions of Table 4 , which analyzes the impact of different combinations of regularization functions.

G Licensing and Third-Party Assets.

Our method builds upon the publicly available TabPFN codebase, which is released under the Apache 2.0 License. All real-world datasets used in the evaluation are sourced from OpenML.org, a platform hosting open datasets for machine learning research; all datasets used are publicly accessible and

Table 12: Synthetic gaussian datasets - Brier

ID	KM	GMM	AE-KM	AE-GMM	DEC	IDEC	G-CEALS	ZEUS
0	<u>0.1448</u>	0.2200	0.1741	0.3558	0.4251	0.3264	0.3921	0.1242
1	0.1218	<u>0.1886</u>	0.2337	0.4718	0.4379	0.4109	0.4377	0.4502
2	0.1985	0.9985	0.2995	0.1922	0.4303	0.2321	0.5400	<u>0.1952</u>
3	<u>0.0528</u>	0.9078	0.0927	0.3012	0.6196	0.1628	0.4194	0.0413
4	0.1005	0.0575	0.1793	0.3351	0.4955	0.2312	0.3886	<u>0.0792</u>
5	<u>0.1020</u>	1.0950	0.1333	0.4892	0.3355	0.2059	0.3995	0.0881
6	0.0350	0.0156	0.1200	0.0489	0.2971	0.0770	0.3561	<u>0.0209</u>
7	<u>0.0632</u>	0.9781	0.1599	0.2610	0.4693	0.1207	0.6146	0.0543
8	<u>0.1168</u>	0.0844	0.2079	0.2786	0.4626	0.2970	0.5975	0.1631
9	0.0677	0.0092	0.3552	0.1925	0.2167	0.2090	0.4586	<u>0.0573</u>
10	0.1091	0.0292	0.1469	<u>0.0460</u>	0.3300	0.1229	0.3127	<u>0.0655</u>
11	0.0558	0.0117	0.0791	0.1370	0.4110	0.1122	0.4437	<u>0.0234</u>
12	0.1361	0.2296	0.4022	0.3492	0.5917	0.3230	0.3583	<u>0.1545</u>
13	<u>0.0216</u>	0.0115	0.0356	0.0629	0.3223	0.0980	0.1947	<u>0.0270</u>
14	<u>0.1048</u>	0.8000	0.3009	0.3776	0.3359	0.2380	0.3818	0.0626
15	0.0734	0.0278	0.2574	0.0746	0.3458	0.2483	0.3120	<u>0.0352</u>
16	<u>0.0537</u>	0.0448	0.0958	0.1747	0.1640	0.2528	0.1454	<u>0.1770</u>
17	<u>0.1309</u>	0.3513	0.4178	0.2891	0.4313	0.2756	0.5425	0.1308
18	<u>0.1035</u>	0.0452	0.1458	0.2319	0.5193	0.2117	0.2961	0.1939
19	<u>0.1475</u>	0.1132	0.3094	0.2989	0.2444	0.4612	0.3015	0.3942
Mean	0.0970	0.3110	0.2073	0.2484	0.3943	0.2308	0.3946	<u>0.1269</u>
Mean-Rank	2.30	3.25	4.55	4.95	6.65	4.85	6.75	<u>2.70</u>
Top-3	19	13	6	2	1	3	0	<u>16</u>
Top-1	2	11	0	1	0	0	0	<u>6</u>

Table 13: Synthetic transformed datasets - Brier

ID	KM	GMM	AE-KM	AE-GMM	DEC	IDEC	G-CEALS	ZEUS
0	0.5116	<u>0.2135</u>	0.6639	0.4457	0.5911	0.5063	0.7116	0.1282
1	<u>0.0666</u>	0.0484	0.2328	0.1514	0.4755	0.5045	0.2806	0.2718
2	0.0883	0.0330	0.4996	0.2822	0.4424	0.3441	0.5990	<u>0.0394</u>
3	0.3254	0.6286	0.5872	0.2118	0.3241	0.4862	0.7537	<u>0.2678</u>
4	0.6757	0.1547	0.5580	0.6123	0.3920	0.5158	0.3804	<u>0.3190</u>
5	<u>0.0887</u>	0.0359	0.3201	0.1517	0.6415	0.4114	0.3869	0.2802
6	<u>0.5771</u>	0.1788	0.4789	0.4049	0.5718	0.3069	0.5448	0.1763
7	0.3634	<u>0.2875</u>	0.4281	0.3326	0.5478	0.3379	0.6068	0.2461
8	0.1048	0.2738	0.1271	0.0817	0.4517	<u>0.0784</u>	0.3278	0.0167
9	0.3014	0.0120	0.3120	0.0940	0.4474	<u>0.3329</u>	0.2284	<u>0.0481</u>
10	0.1785	0.0763	0.3674	<u>0.1249</u>	0.3845	0.5057	0.5420	0.1387
11	<u>0.1053</u>	0.0130	0.1684	0.1128	0.6071	0.2580	0.3306	0.1768
12	<u>0.3682</u>	0.0657	0.6462	0.4740	0.3838	0.4585	0.6318	<u>0.1936</u>
13	<u>0.0604</u>	0.2549	0.4206	0.4292	0.3711	0.4073	0.3436	0.0355
14	<u>0.0445</u>	0.7982	1.1164	0.6259	0.3672	0.4949	0.6715	0.0097
15	<u>0.7142</u>	0.7088	0.6256	0.7924	0.5801	<u>0.5741</u>	0.4807	0.8854
16	<u>0.0524</u>	0.4745	0.1194	0.0303	0.5832	0.1743	0.1014	0.0809
17	0.2586	<u>0.0230</u>	0.2616	0.0394	0.3480	0.2156	0.6361	0.0177
18	<u>0.2081</u>	0.6698	0.3781	0.2409	0.3774	0.3861	0.7879	0.1056
19	0.5120	<u>0.1821</u>	0.7577	0.6415	0.3892	0.4845	0.5570	0.1542
Mean	0.2803	<u>0.2566</u>	0.4535	0.3140	0.4638	0.3892	0.4951	0.1796
Mean-Rank	3.95	<u>3.00</u>	5.85	3.95	5.75	5.00	6.15	2.35
Top-3	9	<u>14</u>	0	12	4	3	2	16
Top-1	0	<u>8</u>	0	2	0	0	1	9

labeled as open data, although individual datasets may be subject to specific licenses (e.g., CC-BY or similar). We ensured that no proprietary or restricted datasets were used. Our released code is provided under the Apache 2.0 License and includes full instructions to reproduce the experiments.

Table 14: Real/OpenML datasets - ablations ARI

ID	\mathcal{L}_{prob}	$\mathcal{L}_{prob} + \mathcal{L}_{sep}$	$\mathcal{L}_{prob} + \mathcal{L}_{cp}$	$\mathcal{L}_{prob} + \mathcal{L}_{sep} + \mathcal{L}_{cp}$
14	48.40	43.49	46.44	50.56
15	<u>86.64</u>	87.17	82.94	81.28
16	69.87	73.33	81.87	<u>74.03</u>
18	43.06	<u>50.80</u>	49.62	51.63
22	<u>63.27</u>	<u>56.86</u>	65.58	56.05
35	52.33	74.58	<u>76.90</u>	85.12
51	32.31	31.54	<u>41.84</u>	43.66
53	5.17	<u>27.38</u>	25.85	35.76
56	58.48	<u>61.34</u>	20.84	66.41
61	48.93	88.57	65.37	<u>85.15</u>
187	<u>88.38</u>	91.50	88.22	<u>88.19</u>
377	46.31	45.16	<u>54.56</u>	55.30
458	98.16	<u>98.49</u>	<u>98.49</u>	99.19
481	2.77	25.87	1.53	<u>8.68</u>
694	<u>42.76</u>	48.86	30.35	33.38
721	43.28	<u>5.39</u>	43.28	43.28
733	34.35	24.94	76.83	<u>74.97</u>
745	<u>59.56</u>	22.80	4.46	73.85
756	76.15	<u>63.49</u>	38.42	50.31
796	6.56	3.96	14.52	<u>13.99</u>
820	39.95	39.95	<u>34.72</u>	28.87
840	0.95	4.13	31.14	<u>27.66</u>
854	12.37	12.37	<u>24.32</u>	76.14
1462	92.00	94.25	62.85	<u>92.28</u>
1495	-0.29	98.40	<u>7.35</u>	<u>7.35</u>
1499	60.63	44.86	<u>71.34</u>	82.40
1510	70.09	<u>73.67</u>	72.51	74.26
1523	<u>25.68</u>	28.13	17.38	19.60
4153	<u>38.28</u>	<u>51.26</u>	50.24	62.29
40496	34.15	<u>33.63</u>	30.68	32.25
40682	-0.39	23.38	42.79	53.15
40705	40.00	<u>40.51</u>	38.18	45.45
42261	48.93	88.57	65.37	<u>85.15</u>
42585	53.97	<u>95.82</u>	97.39	<u>95.05</u>
Mean	44.80	<u>51.60</u>	48.65	57.43
Mean-rank	3.00	<u>2.37</u>	2.68	1.96
Top-3	20	<u>26</u>	25	30
Top-1	2	<u>9</u>	6	15

Broader Impact. Although ZEUS is designed as a general-purpose tool for clustering tabular data, its use in high-stakes domains like healthcare, finance, or criminal justice carries inherent risks. In such contexts, automated grouping of individuals—especially without labels or fairness constraints—can lead to biased or opaque outcomes. We therefore recommend that any deployment of ZEUS in sensitive applications be accompanied by fairness assessment and expert review.

Table 15: Synthetic gaussian datasets - ablations ARI

ID	\mathcal{L}_{prob}	$\mathcal{L}_{prob} + \mathcal{L}_{sep}$	$\mathcal{L}_{prob} + \mathcal{L}_{cp}$	$\mathcal{L}_{prob} + \mathcal{L}_{sep} + \mathcal{L}_{cp}$
0	72.89	68.81	<u>85.85</u>	87.65
1	89.50	71.68	<u>88.72</u>	72.04
2	80.18	63.23	92.59	<u>82.96</u>
3	77.05	79.22	<u>91.23</u>	95.76
4	72.32	84.96	<u>92.82</u>	92.85
5	91.88	88.98	82.25	<u>90.72</u>
6	81.85	81.18	<u>87.49</u>	97.89
7	85.33	79.93	93.75	93.60
8	72.54	76.12	87.92	<u>84.00</u>
9	<u>95.47</u>	95.97	93.59	94.55
10	<u>88.23</u>	89.61	85.07	87.32
11	<u>97.26</u>	94.91	96.55	97.45
12	77.58	78.07	<u>85.81</u>	86.04
13	74.41	76.08	<u>96.07</u>	96.17
14	84.00	82.11	95.39	<u>94.60</u>
15	77.65	78.94	97.10	<u>96.68</u>
16	<u>93.82</u>	93.46	95.82	87.19
17	88.83	86.38	<u>88.05</u>	86.29
18	89.90	90.21	<u>90.02</u>	83.01
19	76.62	<u>77.69</u>	85.63	73.85
Mean	83.37	81.88	90.59	<u>89.03</u>
Mean-rank	2.80	3.00	2.00	<u>2.20</u>
Top-3	14	13	17	<u>16</u>
Top-1	<u>3</u>	<u>3</u>	7	7

Table 16: Synthetic transformed datasets - ablations ARI

ID	\mathcal{L}_{prob}	$\mathcal{L}_{prob} + \mathcal{L}_{sep}$	$\mathcal{L}_{prob} + \mathcal{L}_{cp}$	$\mathcal{L}_{prob} + \mathcal{L}_{sep} + \mathcal{L}_{cp}$
0	67.29	71.62	85.76	87.42
1	<u>91.98</u>	91.46	96.88	89.40
2	93.17	<u>93.84</u>	92.36	95.88
3	68.26	71.68	<u>80.53</u>	80.98
4	80.93	<u>81.64</u>	84.22	73.66
5	81.38	80.06	95.99	<u>81.63</u>
6	84.29	82.06	80.67	87.02
7	83.35	73.07	96.83	<u>89.57</u>
8	97.42	98.61	97.16	<u>98.11</u>
9	97.63	96.43	96.37	<u>97.20</u>
10	91.32	77.37	<u>90.58</u>	86.42
11	91.84	89.07	99.17	<u>93.19</u>
12	74.93	92.20	<u>91.14</u>	<u>87.75</u>
13	0.32	0.73	<u>90.67</u>	91.60
14	98.00	98.83	98.16	<u>98.49</u>
15	43.28	48.54	30.50	28.96
16	93.34	90.38	<u>98.11</u>	99.01
17	<u>97.62</u>	98.21	95.86	96.44
18	<u>82.64</u>	82.22	86.94	79.70
19	77.93	67.71	<u>83.78</u>	84.13
Mean	79.85	79.29	88.58	86.33
Mean-rank	2.80	2.70	<u>2.30</u>	2.20
Top-3	15	14	<u>15</u>	16
Top-1	2	5	<u>6</u>	7